



**AMS**  
American Meteorological Society

## Supplemental Material

© Copyright 2021 [American Meteorological Society](https://www.ametsoc.org) (AMS)

For permission to reuse any portion of this work, please contact [permissions@ametsoc.org](mailto:permissions@ametsoc.org). Any use of material in this work that is determined to be “fair use” under Section 107 of the U.S. Copyright Act (17 USC §107) or that satisfies the conditions specified in Section 108 of the U.S. Copyright Act (17 USC §108) does not require AMS’s permission. Republication, systematic reproduction, posting in electronic form, such as on a website or in a searchable database, or other uses of this material, except as exempted by the above statement, requires written permission or a license from AMS. All AMS journals and monograph publications are registered with the Copyright Clearance Center (<https://www.copyright.com>). Additional details are provided in the AMS Copyright Policy statement, available on the AMS website (<https://www.ametsoc.org/PUBSCopyrightPolicy>).

Supplement for Reconstructing an Interdecadal Pacific Oscillation index from a Pacific Basin-wide collection of ice core records

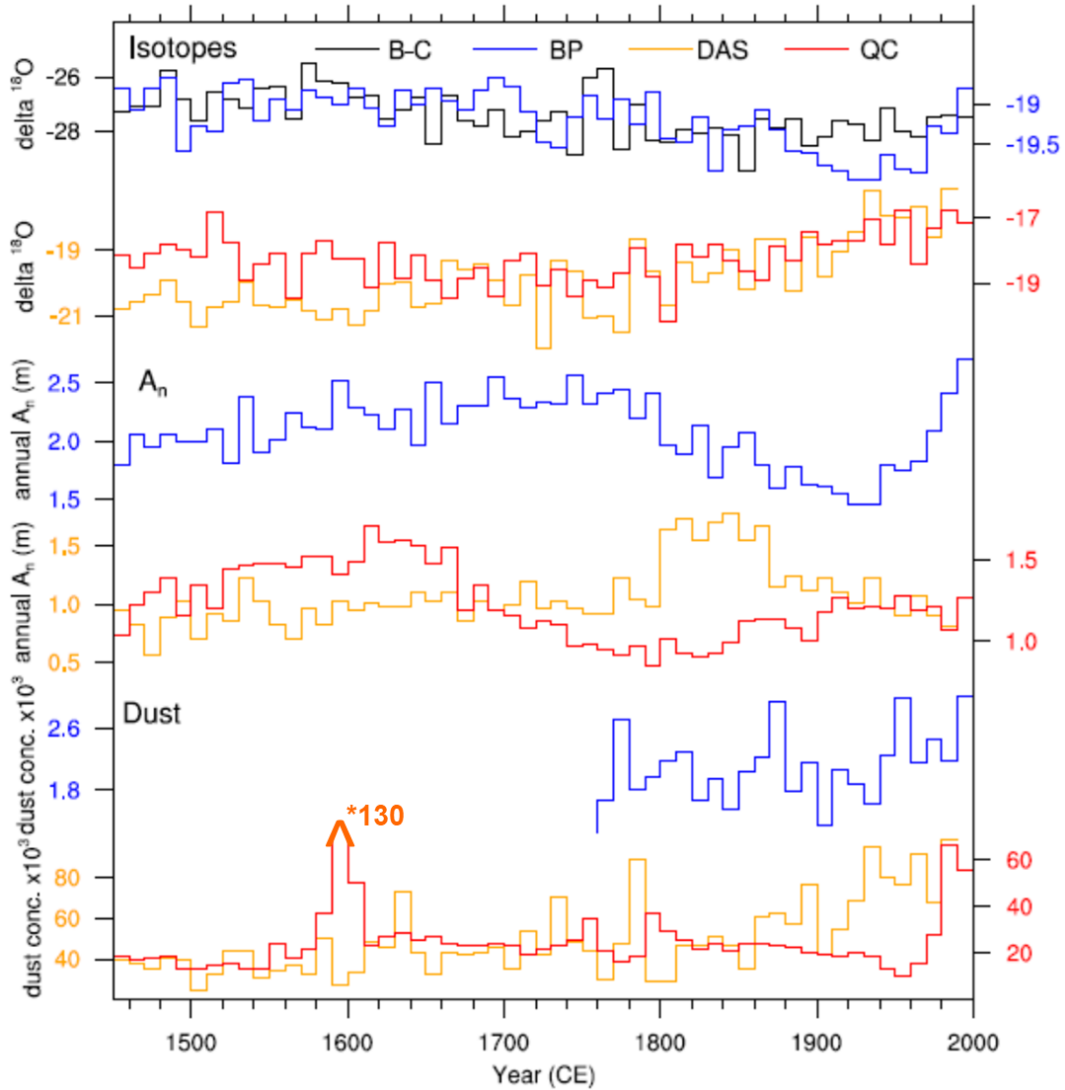


**FIG. S1.** Decadal averages for the ice cores employed in this study including Quelccaya (red; Thompson et al. 2013), Dasuopu (orange; Thompson et al. 2000), Bruce Plateau (blue; Goodwin 2013), and Bona-Churchill  $\delta^{18}\text{O}$  (black; Porter et al. 2019). Accumulation and dust concentrations from Bona-Churchill are available upon request. The asterisk represents the high dust concentrations in the Quelccaya record due to the Huaynaputina eruption in 1600 CE.

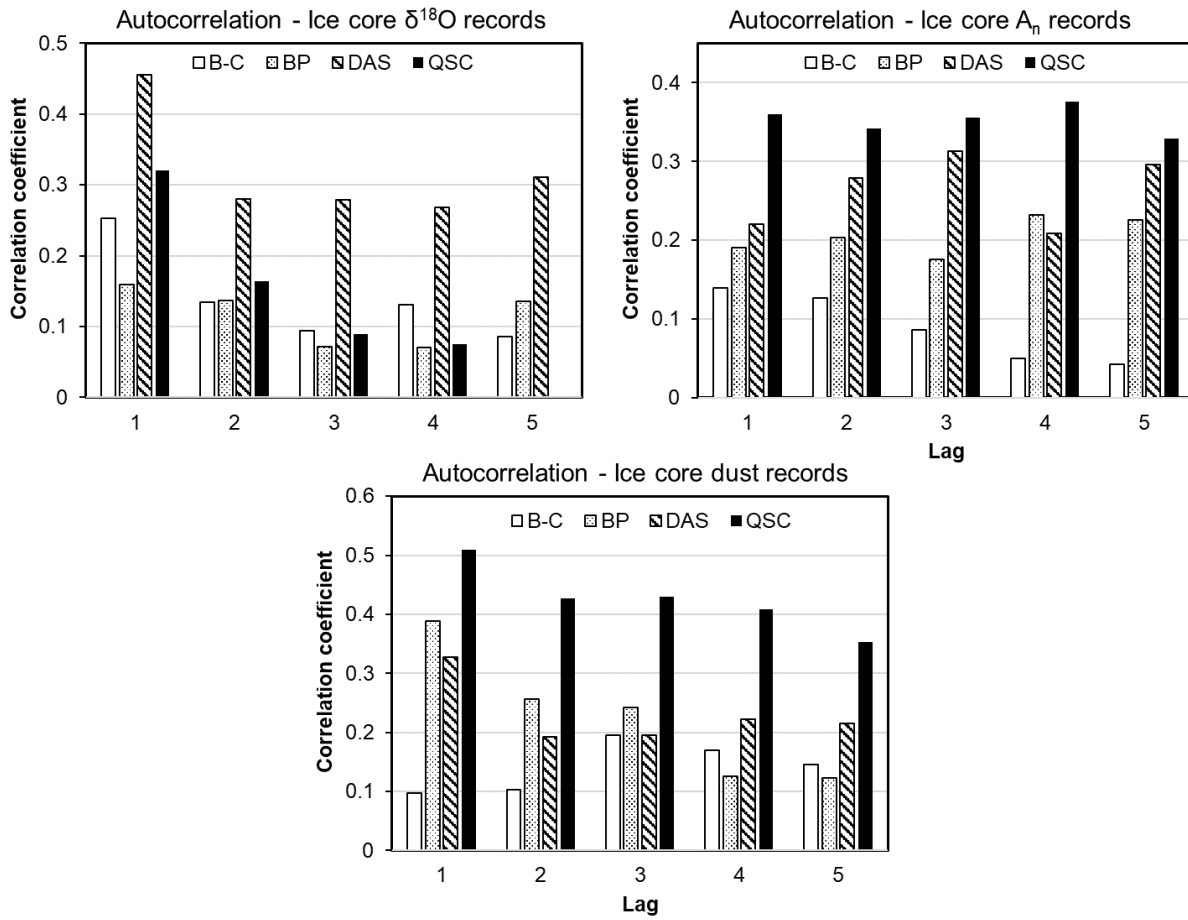


**FIG. S2.** Autocorrelation of the annual ice core records in this study for lags of one to five years.

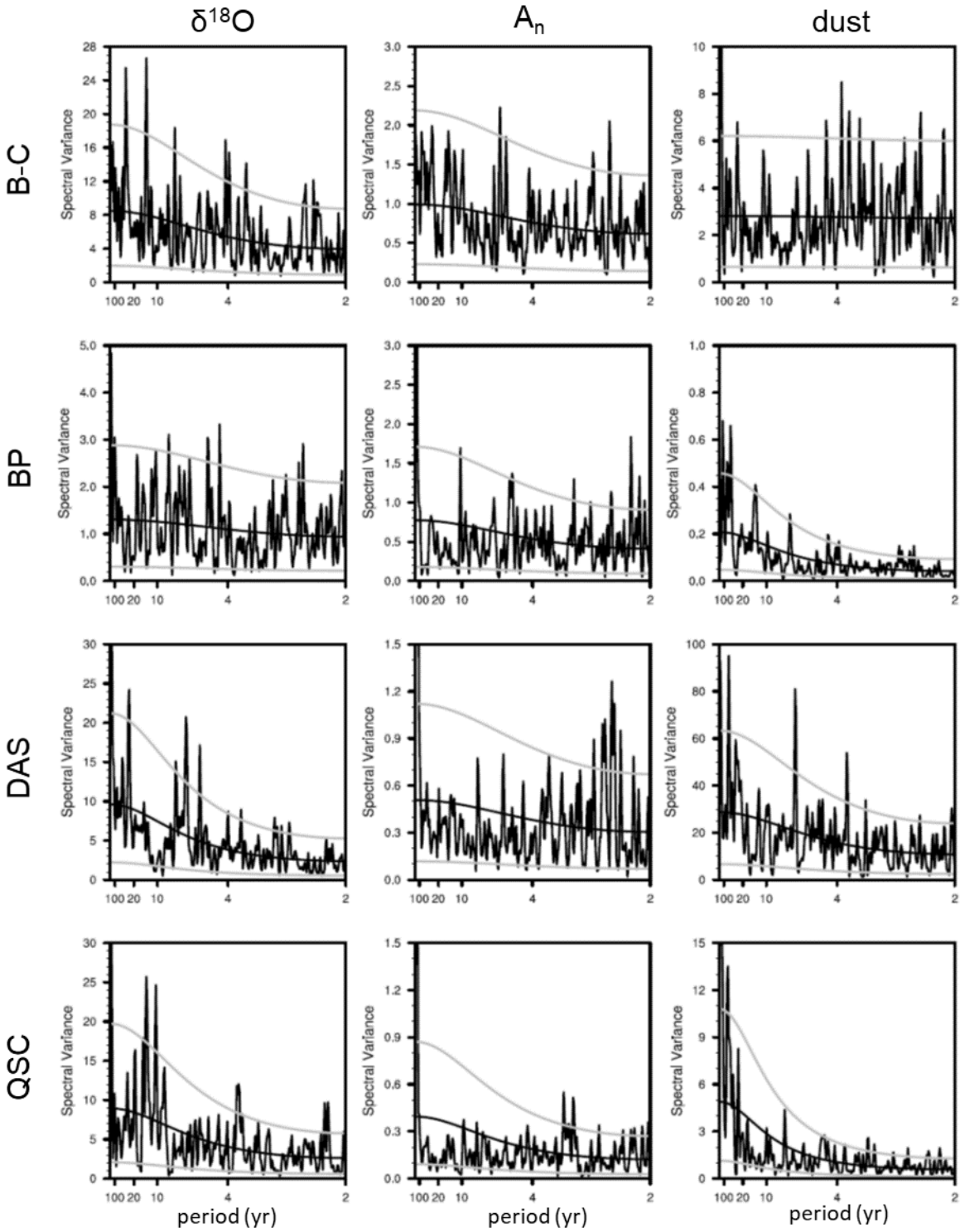


**FIG. S3.** The spectral variance for the ice cores used in this study. The gray lines represent the 5% and 95% confidence intervals around the Markov red noise (black line).

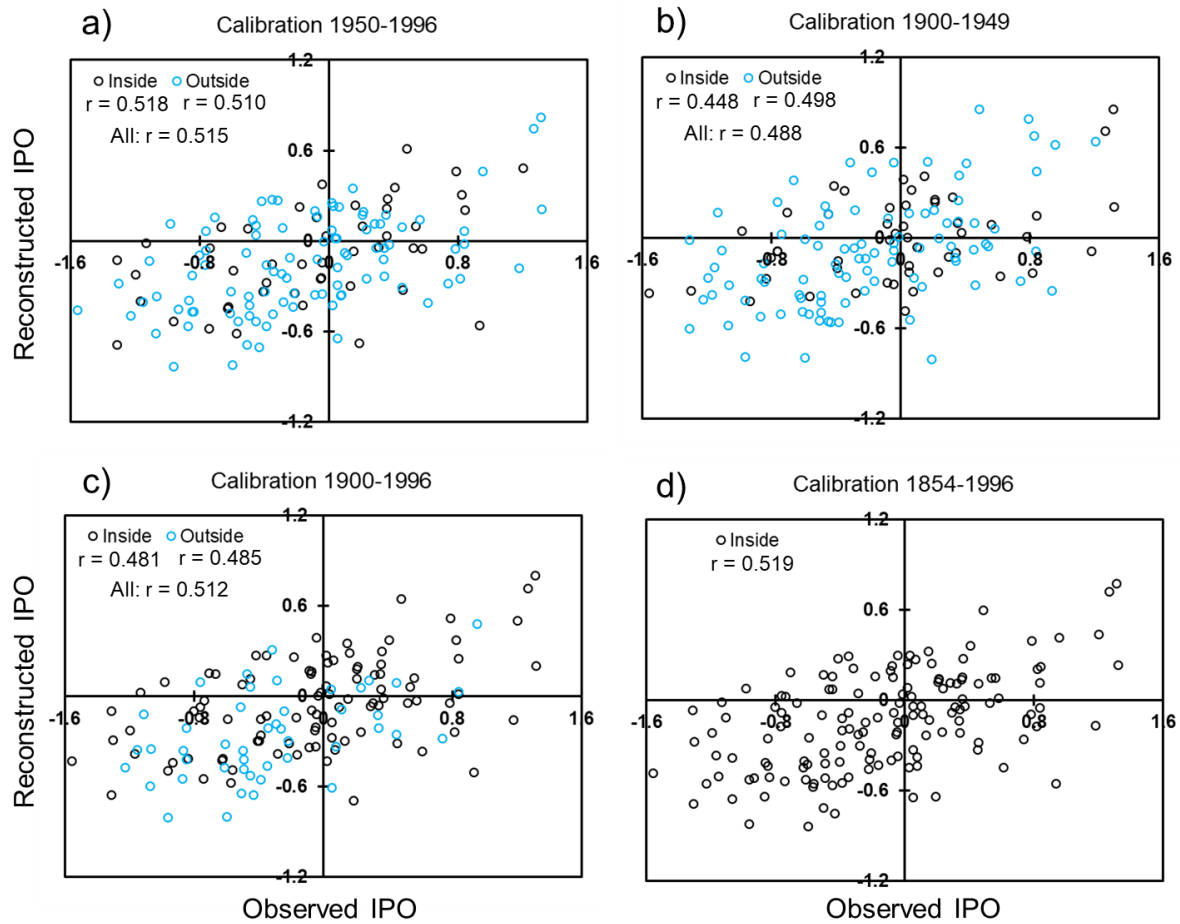


**FIG. S4.** Scatterplot of the observed versus reconstructed IPO for various calibration periods. Relationships are shown between the observed and reconstructed IPO indices for the period 1854-1996 for years within the calibration period (black) and outside of the calibration period (blue). All correlation coefficients are significant at the 99% level ( $p < 0.01$ ). The 1900-1996 calibration period (c) is used for this study.

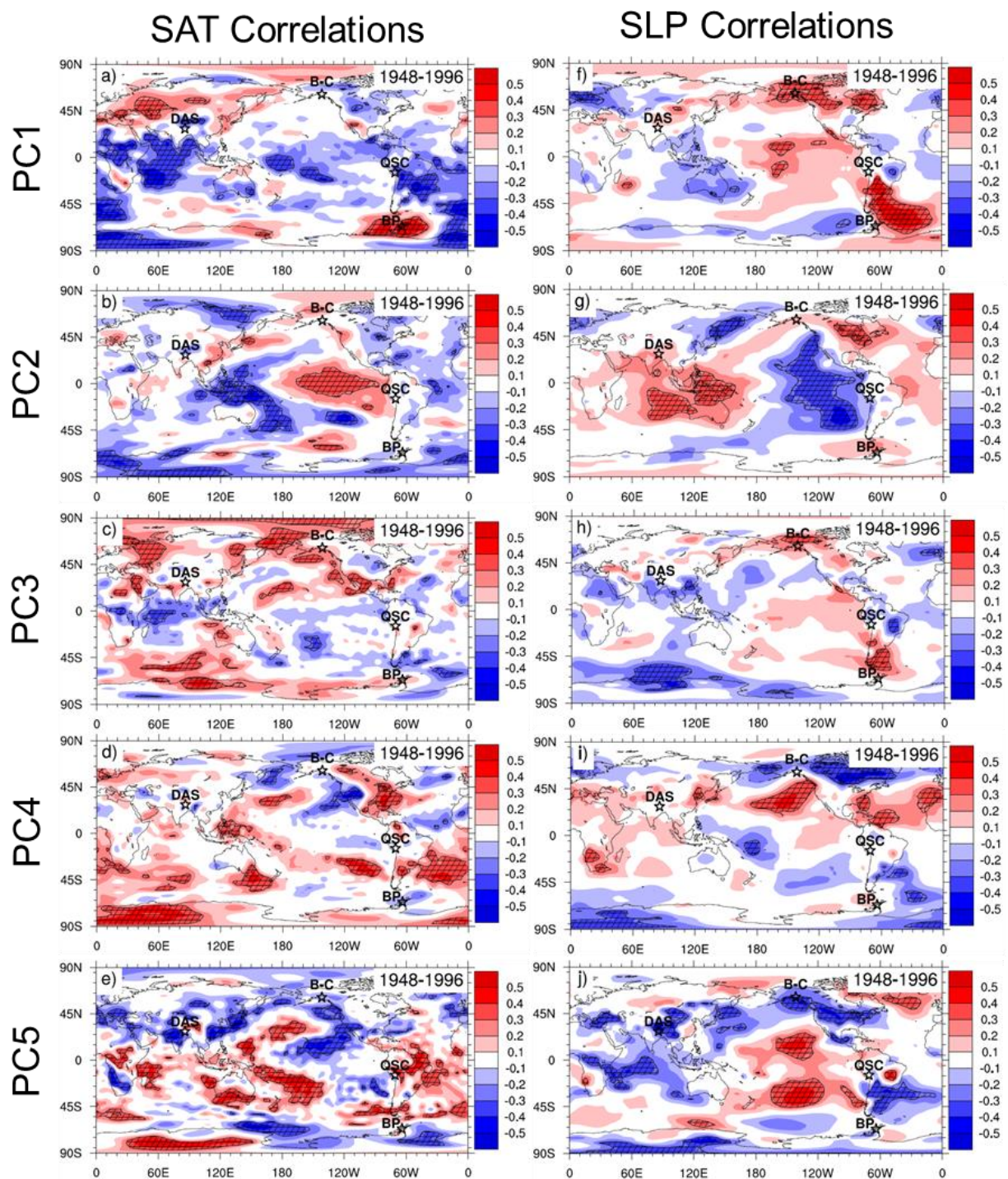


**FIG. S5.** Spatial correlation fields between the five principal components and surface air temperature (SAT; a-e) and sea level pressure (SLP; f-j) from NCEP/NCAR reanalysis for the 1948-1996 period. Data are detrended and hatching indicates 95% significance.

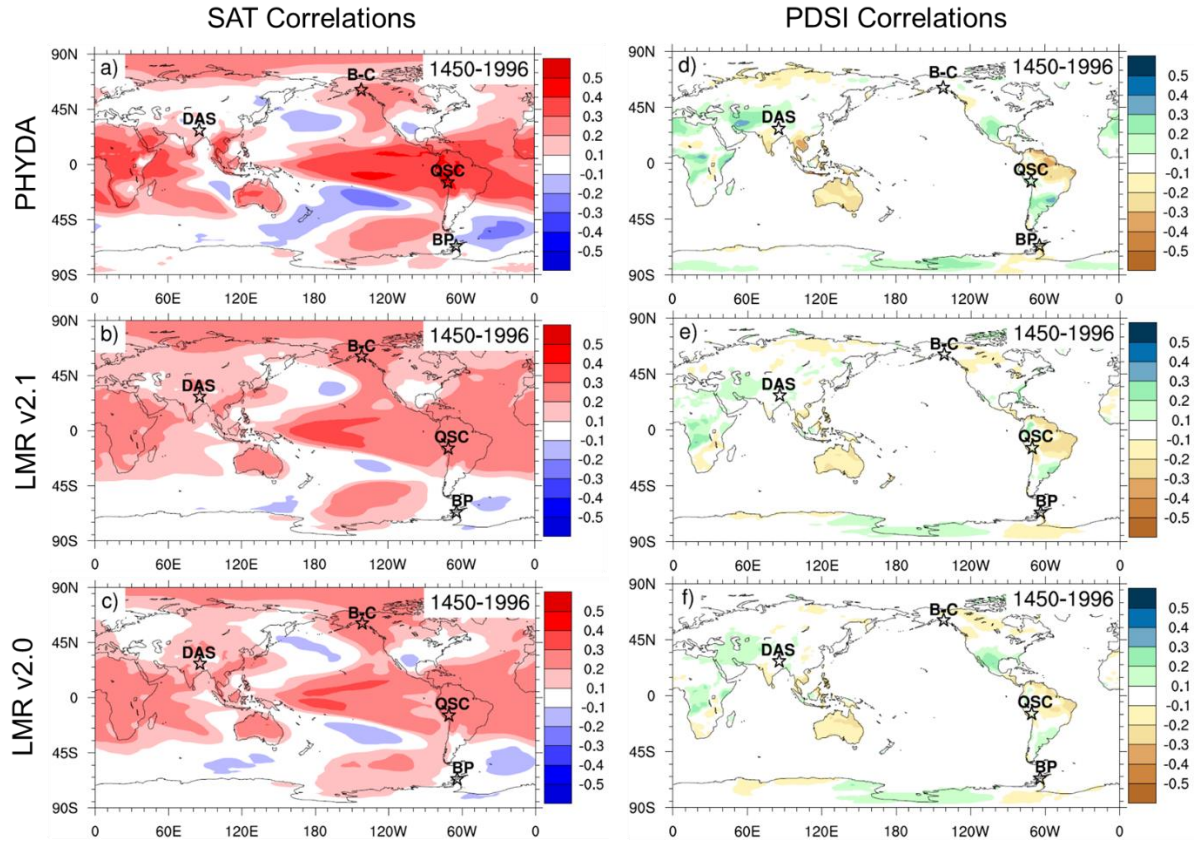


**FIG. S6.** Spatial correlation fields between the reconstructed IPO and (a-c) surface air temperature and (d-f) PDSI from (a, d) PHYDA, (b, e) LMR v2.1, and (c, f) LMRv2.0 for the 1450-1996 CE period. Shading indicates 95% significance.

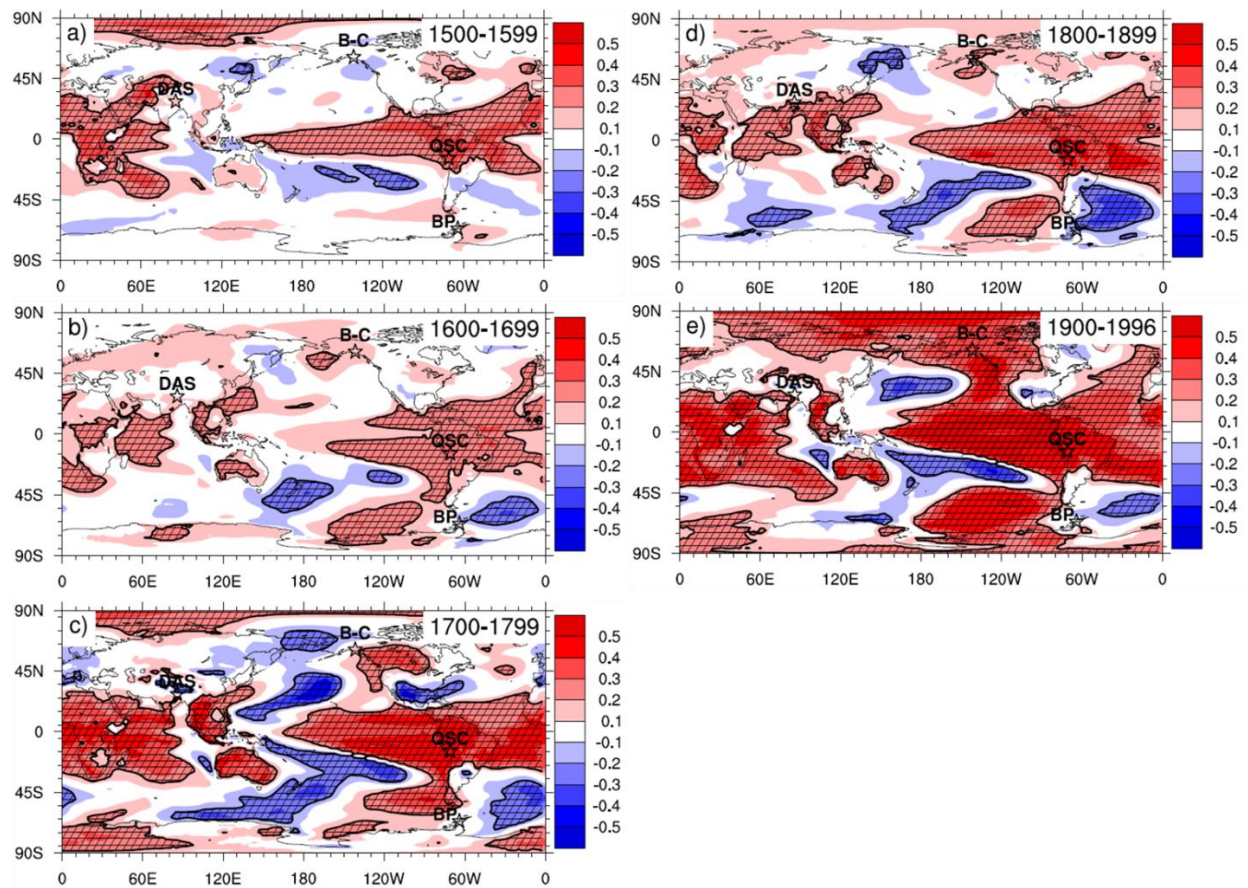


**FIG. S7.** Spatial correlation fields between the reconstructed IPO index and surface air temperature from PHYDA for each century. Hatching indicates 95% significance.



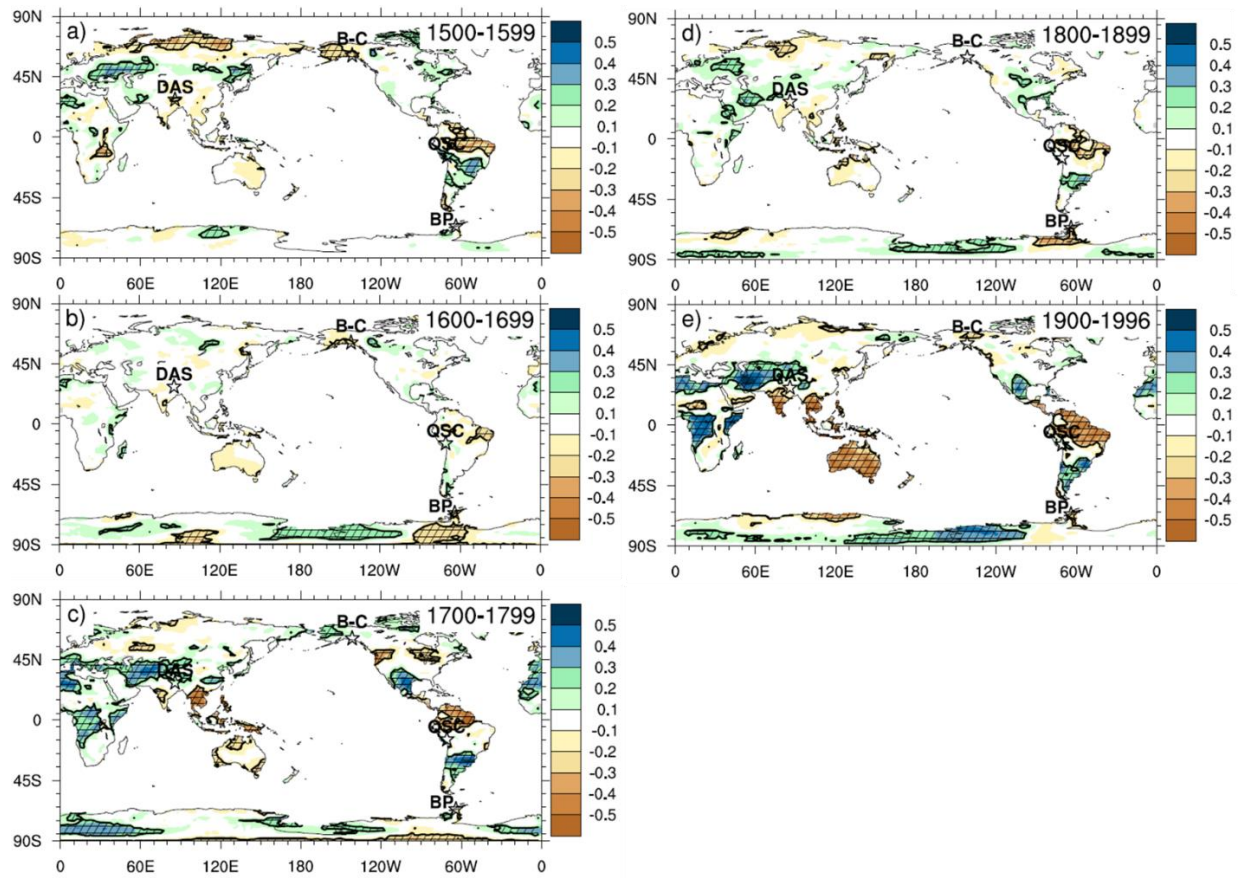


**FIG. S8.** Spatial correlation fields between the reconstructed IPO index and PDSI from PHYDA for each century. Hatching indicates 95% significance.

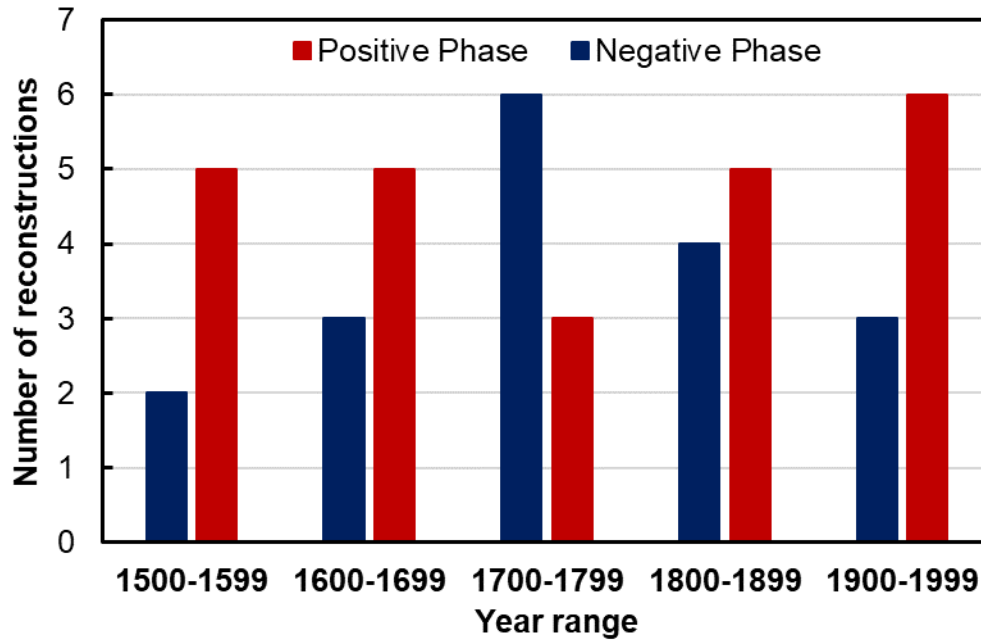


**FIG. S9.** Frequency plot of the predominance of positive (red) and negative (blue) IPO/PDO phases for each century determined from this study and previous reconstructions shown in Fig. 6 of the main text.

**Table S1.** Correlation coefficients for annual ice core data (1450 – 1996 CE). Bold indicates 99% significance.

		BP	DAS	QC	B-C	BP	DAS	QC	B-C	BP	DAS	QC
		$\delta^{18}\text{O}$			$A_n$				Dust			
$\delta^{18}\text{O}$	B-C	0.09	-0.09	0.00	<b>0.18</b>	<b>0.12</b>	<b>-0.13</b>	0.09	<b>-0.21</b>	-0.03	-0.06	0.11
	BP		<b>-0.19</b>	<b>-0.12</b>	-0.01	<b>0.51</b>	-0.09	<b>0.14</b>	-0.05	0.05	<b>-0.21</b>	0.04
	DAS			0.11	<b>0.18</b>	<b>-0.20</b>	0.05	-0.10	<b>0.14</b>	-0.06	<b>0.50</b>	-0.05
	QC				0.07	<b>-0.14</b>	-0.03	-0.07	0.07	0.01	<b>0.17</b>	-0.04
$A_n$	B-C					-0.04	0.03	-0.10	0.04	-0.09	0.09	0.02
	BP						-0.09	0.06	-0.04	0.02	<b>-0.14</b>	<b>0.13</b>
	DAS							<b>-0.15</b>	<b>0.19</b>	-0.04	0.04	-0.05
	QC								<b>-0.20</b>	<b>0.12</b>	-0.06	0.04
Dust	B-C									-0.05	0.05	-0.05
	BP										-0.04	-0.03
	DAS											-0.03

**Table S2.** Loading factors for the first five principal components determined by rotated varimax principal component analysis of four ice core records from 1900 to 1996 CE.

Ice core site	Variable	Principal Component				
		1 (13.4%)	2 (12.7%)	3 (11.7%)	4 (9.8%)	5 (9.5%)
Dasuopu, Tibet	$\delta^{18}\text{O}$	-0.05	0.76	-0.02	-0.03	0.10
	$A_n$	-0.11	-0.32	-0.26	-0.19	0.18
	Dust	-0.07	0.80	-0.04	0.07	0.07
Quelccaya, Peru	$\delta^{18}\text{O}$	-0.29	0.35	0.02	-0.24	-0.52
	$A_n$	0.12	0.10	0.52	-0.16	0.50
	Dust	0.30	-0.15	0.04	-0.16	-0.60
Bona-Churchill, Alaska	$\delta^{18}\text{O}$	0.05	-0.01	0.65	0.44	0.04
	$A_n$	-0.06	0.09	-0.06	0.84	0.01
	Dust	0.04	0.07	-0.80	0.18	0.05
Bruce Plateau, Antarctica	$\delta^{18}\text{O}$	0.83	-0.02	0.06	0.01	-0.02
	$A_n$	0.84	-0.06	-0.00	-0.05	-0.02
	Dust	0.02	0.09	0.01	-0.31	0.46

**Table S3.** Skill statistics for the four different calibration periods

	<b>Skill statistics over the 1854-1996 period</b>			
<b>Calibration Period</b>	1950-1996	1900-1949	1900-1996	1854-1996
<b>Bias</b>	0.002	0.071	0.021	-0.0005
<b>Mean Average Error</b>	0.416	0.427	0.417	0.416
<b>Root Mean Square Error</b>	0.527	0.542	0.528	0.525
	<b>Skill statistics outside of the calibration period</b>			
<b>Calibration Period</b>	1950-1996	1900-1949	1900-1996	1854-1996
<b>Bias</b>	0.004	0.109	0.067	n/a
<b>Mean Average Error</b>	0.417	0.409	0.381	n/a
<b>Root Mean Square Error</b>	0.523	0.528	0.470	n/a

**Table S4.** Years included in the reconstructed and observed IPO composites in Fig. 5

<b>Reconstructed 1450-1996</b>	<b>Years Included</b>
+IPO (+1.5 $\sigma$ ) 35 years total	1451, 1460, 1489, 1504, 1524, 1527, 1530, 1565, 1633, 1634, 1655, 1660, 1722, 1723, 1740, 1763, 1770, 1792, 1794, 1795, 1804, 1825, 1833, 1846, 1880, 1888, 1906, 1940, 1941, 1987, 1990, 1991, 1992, 1993, 1994
-IPO (-1.5 $\sigma$ ) 28 years total	1544, 1547, 1552, 1557, 1587, 1600, 1637, 1662, 1674, 1677, 1691, 1700, 1715, 1717, 1724, 1731, 1778, 1779, 1785, 1786, 1797, 1816, 1819, 1848, 1860, 1874, 1953, 1955
<b>Observed 1948-2018</b>	<b>Years Included</b>
+IPO (10 highest)	1958, 1965, 1969, 1982, 1983, 1987, 1992, 1993, 1997, 2015
-IPO (10 lowest)	1950, 1955, 1956, 1971, 1974, 1975, 1999, 2000, 2008, 2011

**Table S5.** Correlation coefficients between the ice core-derived IPO index from this study and previous reconstructions of Pacific climate variability shown in Fig. 6 of the main text. Bold indicates 99% significance.

<b>Reconstruction</b>	<b>1750 - present</b>	<b>1450 - 1749</b>	<b>1450 - present</b>
Biondi et al. 2001	<b>0.115</b>		
D'Arrigo et al. 2001	<b>0.658</b>		
D'Arrigo and Wilson 2006	-0.107		
Shen et al. 2006	<b>0.237</b>	<b>0.263</b>	<b>0.235</b>
MacDonald and Case 2005	<b>0.161</b>	<b>0.274</b>	<b>0.225</b>
Vance et al. 2015	<b>0.394</b>	-0.041	<b>0.161</b>
LMR v2.0	<b>0.461</b>	-0.110	<b>0.144</b>
Composite	<b>0.399</b>	0.046	<b>0.187</b>

#### REFERENCES

- Biondi, F., A. Gershunov, and D. R. Cayan, 2001: North Pacific decadal climate variability since 1661. *J. Climate*, **14**, 5-10, [https://doi.org/10.1175/1520-0442\(2001\)014<0005:NPDCVS>2.0.CO;2](https://doi.org/10.1175/1520-0442(2001)014<0005:NPDCVS>2.0.CO;2).
- D'Arrigo, R., R. Villalba, and G. Wiles, 2001: Tree-ring estimates of Pacific decadal climate variability. *Climate Dyn.*, **18**, 219-224, <https://doi.org/10.1007/s003820100177>.
- D'Arrigo, R. and R. Wilson, 2006: On the Asian expression of the PDO. *Int. J. Climatol.*, **26**, 1607-1617, <https://doi.org/10.1002/joc.1326>.
- Goodwin, B. P., 2013: Recent environmental changes on the Antarctic Peninsula as recorded in an ice core from the Bruce Plateau. Ph.D. dissertation, Atmospheric Sciences Program, The Ohio State University, 271 pp.  
[http://rave.ohiolink.edu/etdc/view?acc\\_num=osu1373468400](http://rave.ohiolink.edu/etdc/view?acc_num=osu1373468400).

- LMR, 2019: Last Millennium Reanalysis (LMR) Project Global Climate Reconstructions Versions 2 and 2.1, National Centers for Environmental Information, accessed 3 January 2020, <https://www.ncdc.noaa.gov/paleo-search/study/27850>.
- MacDonald, G. M., and R. A. Case, 2005: Variations in the Pacific Decadal Oscillation over the past millennium. *Geophys. Res. Lett.*, **32**, <https://doi.org/10.1029/2005GL022478>.
- NCEP/NCAR, 1996: NCEP/NCAR Reanalysis Monthly Means and Other Derived Variables (updated monthly), NOAA/Earth Systems Research Laboratory/Physical Sciences Laboratory, accessed 22 November 2019, <https://psl.noaa.gov/data/gridded/data.ncep.reanalysis.derived.html>.
- PHYDA, 2018: Paleo Hydrodynamics Data Assimilation product (PHYDA), Zenodo, accessed 1 September 2019, <https://doi.org/10.5281/zenodo.1198817>.
- Porter, S. E., E. Mosley-Thompson, and L. G. Thompson, 2019: Ice core  $\delta^{18}\text{O}$  record linked to Western Arctic sea ice variability. *J. Geophys. Res. Atmos.*, **124**, 10784-10801, <https://doi.org/10.1029/2019JD031023>.
- Shen, C., W-F. Wang, W. Gong, and Z. Hao, 2006: A Pacific Decadal Oscillation record since 1470 AD reconstructed from proxy data of summer rainfall over eastern China. *Geophys. Res. Lett.*, **33**, L03702, <https://doi.org/10.1029/2005GL024804>.
- Thompson, L. G., T. Yao, E. Mosley-Thompson, M. E. Davis, K. A. Henderson, and P.-N. Lin, 2000: A high-resolution millennial record of the South Asian Monsoon from Himalayan ice cores. *Science*, **289**, 1916-1920, <https://doi.org/10.1126/science.289.5486.1916>.

Thompson, L. G., E. Mosley-Thompson, M. E. Davis, V. S. Zagarodnov, I. M. Howat, V. N. Mikhailenko, and P.-N. Lin, 2013: Annually resolved ice core records of tropical climate variability over the past ~1800 years. *Science*, **340**, 945-950, <https://doi.org/10.1126/science.1234210>.

Vance, T. R., J. L. Roberts, C. T. Plummer, A. S. Kiem, and T. D. van Ommen, 2015: Interdecadal Pacific variability and eastern Australian megadroughts over the last millennium. *Geophys. Res. Lett.*, **42**, 129-137, <https://doi.org/10.1002/2014GL062447>.